Arthroplasty Today 14 (2022) 231–236

Contents lists available at ScienceDirect

Arthroplasty Today

journal homepage: http://www.arthroplastytoday.org/

Original research

Attachment and Growth of Fibroblasts and Tenocytes Within a Porous Titanium Scaffold: A Bioreactor Approach

David C. Markel, MD [a, b, c], Paula Dietz, MS [a], Gina Provenzano, MD [a], Therese Bou-akl, MD, PhD [a, b, *], Wei-Ping Ren, MD, PhD [b]

[a] Ascension Providence Hospital, Southfield, MI, USA
[b] Wayne State University, Detroit, MI, USA
[c] The Core Institute, Novi, MI, USA

ARTICLE INFO

Article history:
Received 12 August 2021
Received in revised form
27 September 2021
Accepted 4 December 2021
Available online 15 January 2022

Keywords:
Porous titanium scaffold
Tenocyte
Fibroblast

ABSTRACT

Background: Direct attachment of tendons to metallic implants is important in orthopedics. Tissue integration depends on scaffold microstructure and composition. This study evaluated the effect of pore size of titanium on the viability and function of fibroblasts and tenocytes in a dynamic bioreactor.
Methods: Standardized Ti porous cylinders with 3 pore sizes (400, 700, and 1000 μm) were seeded with fibroblasts or tenocytes (4500 cells/μL) in silicon tubes. Cells were analyzed via alamarBlue (AB) assay in addition to scanning electron microscopy at day 7 (fibroblasts) or day 8 (tenocytes) and day 15. AB functions as a cell health indicator where functional living cells reduce the resazurin dye (blue) in the solution to resorufin (pink), and cell viability can be quantified via spectroscopy.
Results: At day 7, fibroblasts cultured on all sizes reduced AB, with significant differences noted between 400 vs 1000 μm ($P = .013$) and 700 vs 1000 μm ($P = .001$). At day 15, fibroblasts reduced AB on all sizes with a significant difference noted between 700 vs 1000 μm ($P = .004$). Fibroblasts on all 3 pore sizes increased AB reduction from day 7 to day 15. Tenocytes reduced AB with significant differences between the 400 vs 700 μm ($P = .049$) and the 400 vs 1000 μm pore sizes at day 8. In contrast, tenocyte reduction of AB decreased from day 8 to day 15. Scanning electron microscopy performed on fibroblast cylinders showed fibroblasts reached the surface of the cylinders, confirming interconnectivity.
Conclusions: While both fibroblasts and tenocytes penetrated the pores, fibroblasts preferred larger size, whereas tenocytes favored smaller size. Results are encouraging since soft-tissue attachment to a metallic scaffold is difficult but clinically desirable. Future studies could be performed in an in vivo animal model.

Introduction

Tendons are highly ordered structures that transfer forces from muscle to bone to produce motion across a joint. The tendon-bone junction consists of several different cell types including tenocytes, the terminally differentiated cells of a tendon [1]. Tendons are composed mostly of collagen and elastin, which are produced by tenoblasts and tenocytes [2]. If injured, tendons do not fully regenerate their initial properties [3]. Instead, scar tissue forms, which is functionally inferior to native tendon [4]. Tendon injury or rupture around a total joint can be disastrous. For example, repairing the extensor mechanism around a total knee arthroplasty [5-9] or the abductor mechanism around a total hip arthroplasty [10-12] is fraught with error, frequently unsuccessful, and functionally debilitating. When the goal is to achieve attachment of a tendon to an implant surface, there remains a significant mechanical and biologic challenge. With the introduction of porous metallic implants, there was hope that ruptured or resected tendon could be directly reattached to the implant. However, the cellular-metallic pore interaction is not fully understood especially when considering the effect of metallic micropore characteristics on cell penetration and function.

The integration of soft tissue into a substructure depends on the microstructure and composition of the scaffold. Cell ingrowth depends on the porosity, pore size, pore interconnectivity, and the

* Corresponding author. Ascension Providence Hospital, 16001 W Nine Mile Road, Southfield, MI 48075, USA.
E-mail address: therese.bou-akl@ascension.org

https://doi.org/10.1016/j.artd.2021.12.003

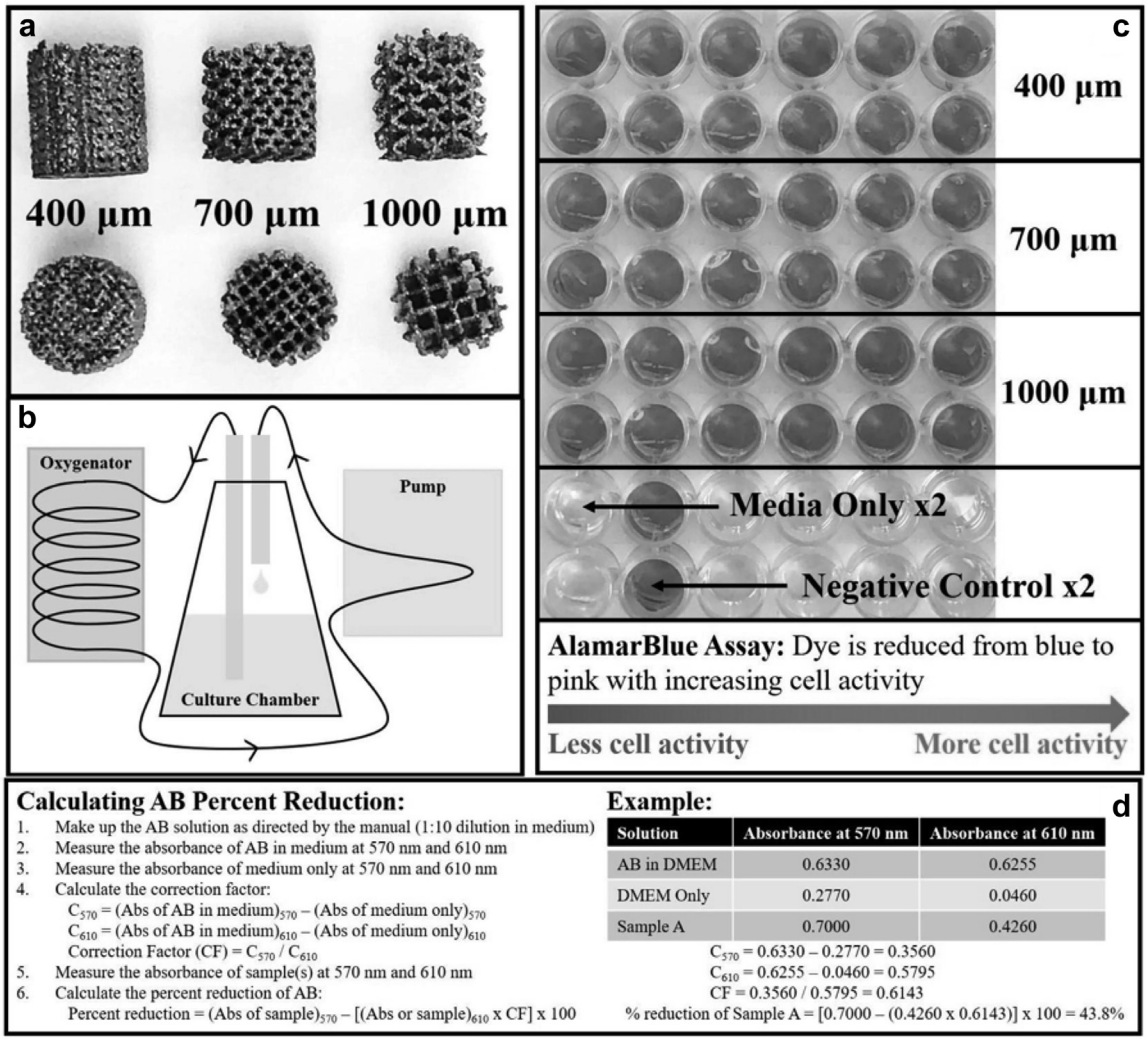

Figure 1. (a) Original cylinders (4 mm long with 4 mm diameter). (b) A sketch of a custom bioreactor with all 3 parts: oxygenator, culture chamber, and pump. (c) Sample of a 96-well plate for AB readings. (d) Sample of AB calculation.

surface characteristics of the implant [13-15]. Titanium (Ti) is a successful implant material, particularly since it is bioinert. There are several in vitro studies on the effect of porosity and/or roughness of Ti scaffolds on cell attachment and function. Blinova et al. found that the irregular porosity of Ti implants induced optimal human dermal fibroblasts and rabbit bone marrow stromal cell proliferation [16]. Oates found that surface roughness and wettability of Ti scaffolds affected the attachment and function of fibroblasts [17]. Borsari et al. found that MG63 osteoblast-like cells proliferated and functioned better on the ultra-high-roughness and ultra-high-dense Ti surface (PG60) than medium TI01 and high TI60 roughness and open porous coatings [18].

Most in vitro cell culture studies were performed under static conditions with cells seeded on the surface of the material tested. Biomedical engineering literature showed that cells proliferated and functioned better when grown under dynamic vs static conditions especially for three-dimensional matrices or scaffolds. Dynamic culture conditions are achieved using bioreactors and continuous medium flow that enhances nutrient and oxygen transport in the culture system [19-21]. Dolder et al. have shown that using a dynamic culture system enhanced the proliferation and matrix production of bone marrow cells seeded in Ti fiber mesh [22]. Also, modifications of the flow and medium conditions in the bioreactor system have been shown to affect the distribution of extracellular matrix within the 3-D Ti mesh [23]. A specific bioreactor design can be used to replicate an in vivo environment [24].

This study was undertaken to evaluate the effects of Ti pore size on cellular behavior. We evaluated the impacts of 3-D printed Ti cylinders with different pore sizes on the attachment and growth of fibroblasts and tenocytes in vitro using a bioreactor approach. Viability and function of cells are compromised in 3-D constructs when the cells are 200-300 µm away from a nutrient source. Therefore, a dynamic culture bioreactor was used to provide an adequate nutrient and oxygenation supply for the cells within the porous structures. We hypothesize that a specific pore size could better encourage soft-tissue ingrowth into a metallic implant.

Material and methods

Ti cylinders

Custom Ti cylinders, with 3 different pore sizes (400, 700, and 1000 µm) were obtained from Stryker Orthopedics (Mahwah, NJ). Pore sizes were selected based on a range that was manufacturable while also encompassing the ranges used for ingrowth devices. Cylinders measured 4 mm in length and 4 mm in diameter (Fig. 1a).

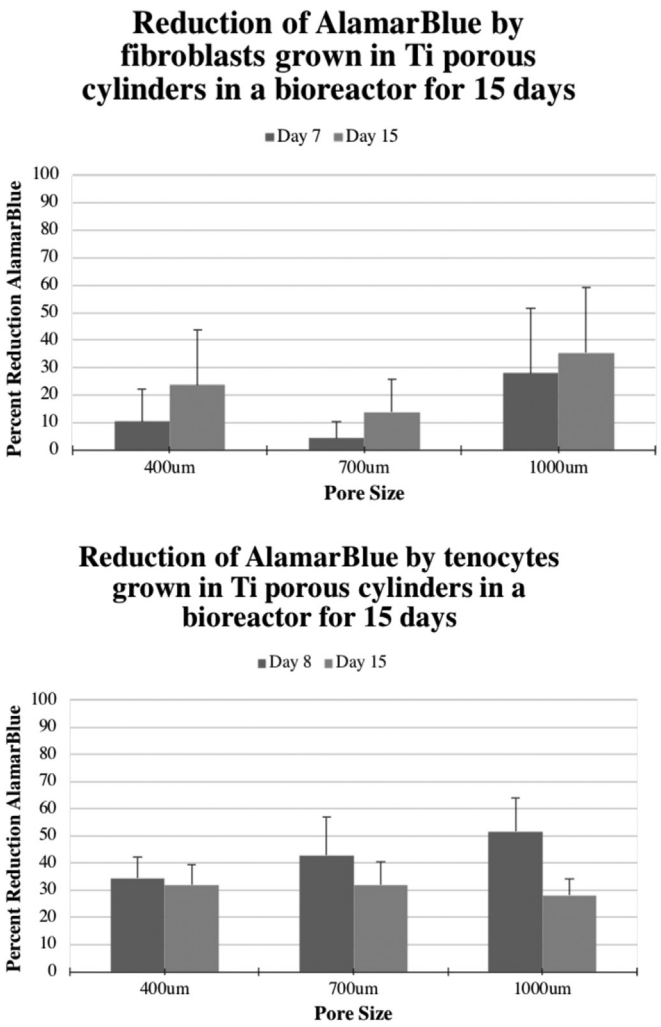

Figure 2. Graph of percent reduction of alamarBlue by fibroblasts and tenocytes at 7 (or 8) and 15 days when cultured in a bioreactor.

To remove any free particles (*residue*), the cylinders were washed in 70% ethanol by stirring for 30 minutes, followed by rinsing with distilled water. Cylinders were then tightly fit into silicone tubing, approximately 12 mm in length and autoclave sterilized.

Custom bioreactor

The bioreactor consisted of 3 main parts: a pump, a culture chamber, and an oxygenator (Fig. 1b). The culture chamber and oxygenator were kept in the incubator during culture at 37°C, while approximately 2 feet of tubing extended out of the incubator connecting it to the pump. Additional details regarding the customization of the bioreactor are described in the Appendix.

Cell preparation and seeding

Early passage human primary dermal fibroblasts (ATCC, Manassa, Virginia; PCS-201-012) and laboratory-isolated tenocytes from Sprague Dawley rats were used in seeding the Ti cylinders [25]. When cells reached confluency, they were trypsinized, counted, and concentrated to approximately 4500 cells per microliter.

Using disposable 1-mL syringes, approximately 90,000 cells were injected into each Ti cylinder and incubated for 2-3 hours at 37°C with 5% CO_2 to allow cell attachment. The Ti cylinders were then transferred to the custom-made bioreactor culture chamber and cultured under dynamic conditions (circulating 50 mL media at 1.3 mL/min) for up to 15 days with full medium change weekly.

alamarBlue Assay

During the culture period, cell viability and function could be analyzed via alamarBlue (AB) assay. AB functions as a cell health indicator where functional living cells reduce the resazurin dye (blue) in the solution to resorufin (pink), and cell viability can be quantified via spectroscopy. Cylinders were removed from the bioreactor at 7 (fibroblasts) or 8 (tenocytes) days and cultured for 24 hours with a medium containing 10% AB substrate. Different days were chosen because of laboratory workflow restrictions. After culture with AB, 100 μl was transferred to a 96-well plate for reading (Fig. 1c), and the cylinders are returned to the bioreactor and cultured until 15 days after seeding. Cylinders were again removed and cultured with AB for a second reading at 15 days. Comparing AB readings from day 7 (or 8) to those from day 15 was performed to determine cell viability and growth. We aimed for approximately 5 cylinders of each pore size with each cell type. In some instances, there was not enough cells to load equal numbers of cylinders, resulting in a sample range of 13-17.

Absorbance was measured by a microplate reader (Synergy HT Multi-Mode Microplate Reader; BioTek Instruments, Winooski, Vermont) at 570 nm and 610 nm. To calculate the percent reduction, a correction factor was needed to adjust the data set around the absorbance of the fully oxidized form of AB in various media (presence of phenol red). The raw absorbance values were calculated as shown in Figure 1d.

Scanning electron microscopy

At the end of each culture, the seeded cylinders were fixed in 70% ethanol for at least 24 hours. Before scanning, they were air dried overnight and the surface scanned using an environmental scanning electron microscope (ESEM; Quanta 450FEG). Images

Table 1
Average percent reduction (and standard deviation) of alamarBlue by fibroblasts and tenocytes at 7 (or 8) and 15 days when cultured in a bioreactor.

Cell type	Pore size (μm)	% Reduction at 7 (or 8) d (±standard deviation)	% Reduction at 15 d (±standard deviation)	*P*-value
Fibroblasts	400	10.54 (±11.81)	23.70 (±20.02)	.028[b]
	700	4.30 (±6.17)	13.91 (±11.95)	.010[b]
	1000	28.09 (±23.36)	35.36 (±23.94)	.392[b]
	P value	<.001[a]	.011[a]	
Tenocytes	400	34.51 (±7.69)	31.97 (±7.49)	.376[b]
	700	42.91 (±14.13)	32.06 (±8.32)	.013[b]
	1000	51.60 (±12.42)	28.15 (±6.04)	<.001[b]
	P value	.002[a]	.302[a]	

[a] Statistics performed by one-way analysis of variance.
[b] Statistics performed by two-tailed T-test.

Table 2
P values for pore size comparisons at each time point.

Cell type	Pore size (um)	*P* value on d 7 (or 8)	*P* value on d 15
Fibroblasts	400 vs 700	.085	.101
	400 vs 1000	**.010**	.139
	700 vs 1000	**.001**	**.003**
Tenocytes	400 vs 700	.051	.976
	400 vs 1000	**<.001**	.159
	700 vs 1000	.094	.168

Bold indicates statistics were performed by two-tailed post hoc T-test with Bonferroni correction.

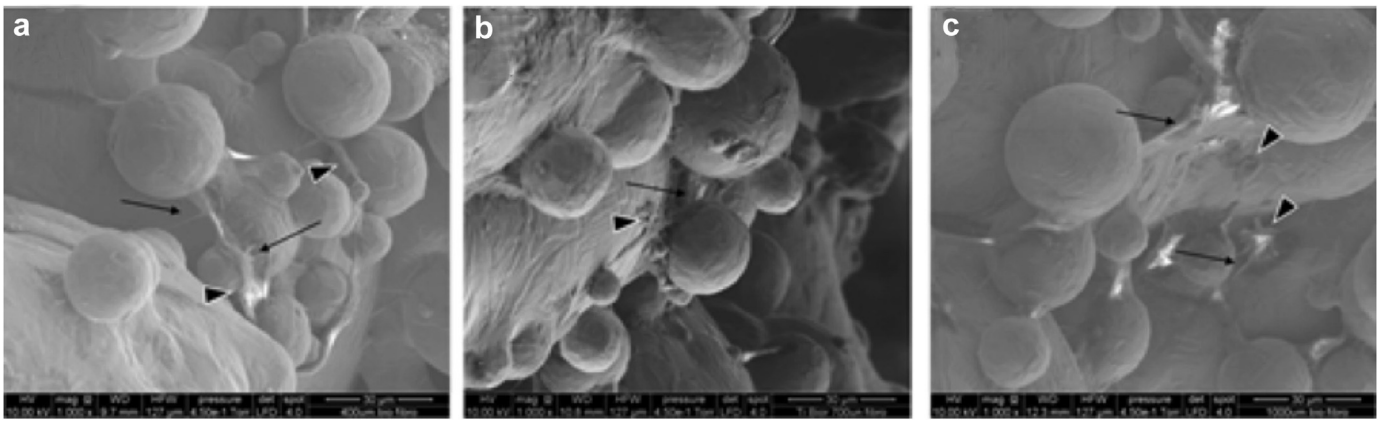

Figure 3. Fibroblast attachment on cylinders with pore diameters 400 μm (a), 700 μm (b), and 1000 μm (c) at 1000× magnification. Arrowheads show cell bodies, and arrows show cellular extensions.

were captured to show the morphology of attached cells on the surface of the porous material.

Statistical analysis

Three independent trials with each cell type were performed (total n = 13-17 for each pore size). Using the Microsoft Excel data analysis tool pack, one-way analysis of variance and paired two-tailed T-tests were used to compare AB data for all pore sizes. *P* values less than .05 was considered significant.

Results

At day 7, fibroblasts cultured on the 400-, 700-, and 1000-μm pore size Ti cylinders reduced AB by 11%, 4%, and 28% (Fig. 2), respectively; significant differences were noted between the 400 vs 1000 μm ($P = .010$) and the 700 vs 1000 μm ($P = .001$) pore sizes but no differences between 400 vs 700 μm ($P = .085$) (Table 2). At day 15, fibroblasts cultured on the 400-, 700-, and 1000-μm pore size cylinders reduced AB by 24%, 14%, and 35%, respectively; significant differences were noted between 700 vs 1000 μm ($P = .003$), but not between the other pore sizes, 400 vs 700 μm ($P = .101$) and 400 vs 1000 μm ($P = .139$).

Fibroblasts grown on all 3 pore sizes showed increased AB reduction from day 7 to day 15 (Fig. 2). Fibroblasts grown on the 400-μm pore size cylinders reduced AB by 11% on day 7 and by 24% on day 15; this is a significant increase in AB reduction ($P = .028$) (Table 1). On the 700-μm cylinders, the cells reduced AB by 4% on day 7 and by 14% on day 15, also a significant difference ($P = .010$). Although there was an increase in AB reduction on the 1000-μm pore size cylinders at day 7 and day 15, 28% and 35%, respectively, this was not a significant difference ($P = .392$).

On day 8, the tenocytes cultured on the 400-, 700-, and 1000-μm pore size Ti cylinders reduced AB by 35%, 43%, and 52% (Fig. 2), respectively. There was a significant difference between 400 vs 1000 μm ($P < .001$) but not between 400 vs 700 μm ($P = .051$) or 700 vs 1000 μm ($P = .094$) (Table 2). On day 15, the tenocytes reduced AB by 32%, 32%, and 28% for the 400-, 700-, and 1000-μm pores sizes, respectively. No significant differences were noted.

In contrast to the fibroblast cells, tenocyte reduction of AB decreased from day 8 to day 15 (Fig. 2). When grown on the 400-μm pore size cylinders, tenocytes reduced AB by 35% at day 8 and by 32% at day 15 ($P = .376$). For the 700-μm cylinders, AB reduction was 43% on day 8 and 32% on day 15, a significant decrease in reduction ($P = .013$). Similarly, when tenocytes were grown on the 1000-μm pore size cylinders, AB reduction at day 8 was 52% and decreased to 28% by day 15 ($P < .001$).

ESEM was performed on fibroblast- and tenocyte-seeded cylinders for each pore size and showed that some cells had reached

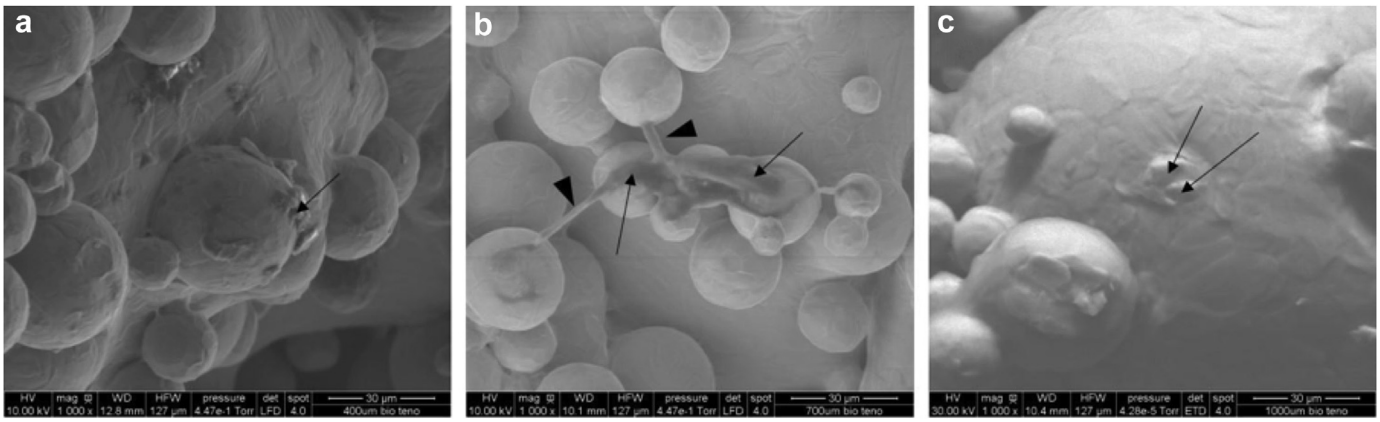

Figure 4. Tenocyte attachment on cylinders with pore diameters 400 μm (a), 700 μm (b), and 1000 μm (c) at 1000× magnification. Arrowheads show cell bodies, and arrows show cellular extensions.

the outer surface of the cylinders, thus confirming the interconnectivity of the pores and that those cells attached and spread on the surface. There was some difference in the cell bodies of the attached cells. The fibroblasts were more elongated while the tenocytes were more rounded (Figs. 3 and 4).

Discussion

There is a clinical need in orthopedic surgery for the ability to attach tendons directly to metallic implants. The mechanical and biologic mechanisms to achieve this attachment are yet unclear. With the advent of printed Ti technology, there is an ability to specifically define the pore size in any particular area of an implant. We hypothesize that defining a specific pore size or potentially even a defined variable or graded pore size could better encourage soft-tissue ingrowth into a metallic implant. Tendon biology is complex. We chose to begin our investigations using 2 different cell types, fibroblasts and tenocytes. Our study purpose was to evaluate the effect of specific pore sizes of 3-D printed Ti cylinders on the viability and function of fibroblasts and tenocytes. Both fibroblasts and tenocytes penetrated the pores and readily attached to the printed Ti material (Fig. 2). The fibroblasts had a preference to grow within the larger pore sizes and had significantly more living cells in the 700- and 1000-μm porous Ti. Based on the cell growth pattern, the interconnectivity of the pores was confirmed by ESEM imaging. During seeding, the outer surface of the cylinders was blocked by silicone tubing. Hence, cells shown on the surface after removal of the tube either proliferated or traveled through the open pores during seeding.

The key point herein was that the individual cell types had preference for different pore sizes within the same substrate, a printed Ti surface. Additional studies would be required to assess the impact of factors such as the addition of growth factors including conditioned media from bone marrow stem cells as well as the effect of combining cells into porous cylinder in the bioreactor setting.

The observed decrease of AB reduction by tenocytes from day 8 to day 15 (Fig. 2) suggested a decline in cell proliferation or an increase in cell death. One potential reason could be related to the low seeding density relative to the available surface area within the cylinders and that these cells may require closer contact for survival. A previous study using a collagen-glucosaminoglycan scaffold found that higher crosslinking densities and smaller pore sizes were able to maintain tenogenic gene expression profiles [26]. This could explain the more profound decrease on the 700-μm and 1000-μm samples or could be related to cell passage and source (primary vs cell line).

A limitation of this study was the fact that we studied the cell types independently. In addition, the pores while defined in size and shape were not “optimized” for any cell type. As an example, Zhao et al. found that the pore shape tetrahedron vs octahedron affected spreading of MC3T3-E1 cells in vitro [27]. The cells spread better on the scaffolds with the octahedron unit [27]. Another limitation of the study was that human fibroblasts were used while tenocytes were harvested from Sprague Dawley rats. For optimal application of how this concept would be applicable in orthopedics, human tenocytes would need to be considered in the future especially if dual cell types were to be studied together.

The results of this study suggest that tenocytes and fibroblasts can grow into a 3-D printed Ti substrate and each cell type has a preferential pore size. This work highlighted the differing behavior of living cells relative to a 3-D printed Ti substrate. This and future work may help to determine the specific structure that would best promote tendon healing into an implant clinically because 3-D printing of orthopedic materials is becoming common. It would be possible to make the porous structure most advantageous to tendon ingrowth situated at the point of tendon repair such as at the greater trochanter or at the tibial tubercle.

Conclusions

While both fibroblasts and tenocytes penetrated the pores, fibroblasts preferred the 1000 μm pore size, whereas tenocytes favored smaller pore size. Although this is a small sample size, results are encouraging because soft-tissue attachment to a metallic scaffold is difficult but clinically desirable. Future studies could be performed in an in vivo animal model.

Conflicts of interest

The authors declare the following financial interests/personal relationships which may be considered as potential competing interests: Dr. D. C. Markel is a paid consultant for Stryker and Smith and Nephew unrelated to this study; has stock or stock options in Arboretum Ventures and HopCo; receives research support from OREF and Stryker; is a board member of Michigan Arthroplasty Registry Collaborative Qualitative Initiative (MARCQI).

For full disclosure statements refer to https://doi.org/10.1016/j.artd.2021.12.003.

Acknowledgments

The authors would like to acknowledge Dr. Yawen Li from Lawrence Technological University for providing the ESEM and for her assistance during the imaging.

References

[1] Benjamin M, Evans EJ, Copp L. The histology of tendon attachments to bone in man. J Anat 1986;49:89.
[2] Kannus P. Structure of the tendon connective tissue. Scand J Med Sci Sports 2000;10(6):312.
[3] Rotini R, Fini M, Giavaresi G, et al. New perspectives in rotator cuff tendon regeneration: review of tissue engineered therapies. Chir Organi Mov 2008;91:87e92.
[4] Freedman BR, Fryhofer GW, Salka NS, et al. Mechanical, histological, and functional properties remain inferior in conservatively treated Achilles tendons in rodents: long term evaluation. J Biomech 2017;56:55.
[5] Bates M, Springer B. Extensor mechanism disruption after total knee arthroplasty. J Am Acad Orthop Surg 2015;23:95.
[6] Courtney PM, Edmiston TA, Pflederer CT, et al. Is there any role for direct repair of extensor mechanism disruption following total knee arthroplasty? J Arthroplasty 2018;33(7S):S244.
[7] Parker DA, Dunbar MJ, Rorabeck CH. Extensor mechanism failure associated with total knee arthroplasty: prevention and management. J Am Acad Orthop Surg 2003;11:238.
[8] Maffulli N, Spiezia F, La Verde L, et al. The management of extensor mechanism disruption after total knee arthroplasty: a systematic review. Sports Med Arthrosc Rev 2017;3(25):41.
[9] Browne JA, Hanssen AD. Reconstruction of patellar tendon disruption after total knee arthroplasty. J Bone Joint Surg Am 2011;93(12):1137.
[10] Weber M, Berry D. Abductor avulsion after primary total hip arthroplasty: results of repair. J Arthroplasty 1997;2(2):202.
[11] Iorio R, Healy WL, Warren PD, Appleby D. Lateral trochanteric pain following primary total hip arthroplasty. J Arthroplasty 2006;21(2):233.
[12] Lübbeke A, Kampfen S, Stern R, Hoffmeyer P. Results of surgical repair of abductor avulsion after primary total hip arthroplasty. J Arthroplasty 2008;23(5):694.
[13] Kapat K, Srivas PK, Rameshbabu AP, et al. Influence of porosity and pore-size distribution in Ti6Al4 V foam on physicomechanical properties, osteogenesis, and quantitative validation of bone ingrowth by micro-computed tomography. ACS Appl Mater Inter 2017;9(45):39235.
[14] Feller L, Jadwat Y, Khammissa RA, et al. Cellular responses evoked by different surface characteristics of intraosseous titanium implants. Biomed Res Int 2015;2015:171945.
[15] El Sayegh TY, Pilliar RM, McCulloch CA. Attachment, spreading, and matrix formation by human gingival fibroblasts on porous-structured titanium alloy and calcium polyphosphate substrates. J Biomed Mater Res 2002;61(3):482.

[16] Blinova MI, Yudintzeva NM, Nikolaenko NS, et al. Cell cultivation on porous titanium implants with various structures. Cell Tissue biol 2010;4(6):572.
[17] Oates CJ, Wen W, Hamilton DW. Role of titanium surface topography and surface wettability on focal adhesion kinase mediated signaling in fibroblasts. Materials (Basel) 2011;4(5):893.
[18] Borsari V, Giavaresi G, Fini M, et al. Comparative in vitro study on a ultra-high roughness and dense titanium coating. Biomaterials 2005;26(240):4948.
[19] Gaspar DA, Gomide V, Monteiro FJ. The role of perfusion bioreactors in bone tissue engineering. Biomatter 2012;2(4):167.
[20] Sailon AM, Allori AC, Davidson DH, et al. A novel flow-perfusion bioreactor supports 3D dynamic cell culture. Biomed Res Int 2009;2009:873816.
[21] Goldstein AS, Juarez TM, Helmke CD, et al. Effect of convection on osteoblastic cell growth and function in biodegradable polymer foam scaffolds. Biomaterials 2001;22:1279.
[22] Van den Dolder J, Bancroft GN, Sikavitsas VI, et al. Flow perfusion culture of marrow stromal osteoblasts in titanium fiber mesh. J Biomed Mater Res A 2003;64(2):235.
[23] Sikavitsas VI, Bancroft GN, Holtorf HL, et al. Mineralized matrix deposition by marrow stromal osteoblasts in 3D perfusion culture increases with increasing fluid shear forces. Proc Natl Acad Sci U S A 2003;100(25):14683.
[24] Selden C, Fuller B. Role of bioreactor technology in tissue engineering for clinical use and therapeautic target design. Bioengineering 2018;5(2):32.
[25] Gungormus C, Kolankaya D, Aydin E. Histopathological and biomechanical evaluation of tenocyte seeded allografts on rat Achilles tendon regeneration. Biomaterials 2015;51:108.
[26] Grier WK, Ehiremen MI, Harley BA. The Influence of proe size and stiffness on tenocyte bioactivity and transcriptomic stability in collagen-GAG scaffolds. J Mech Behav Biomed Mater 2017;65:295.
[27] Zhao D, Huang Y, Ao Y, et al. Effect of pore geometry on the fatigue properties and cell affinity of porous titanium scaffolds fabricated by selective laser melting. J Mech Behav Biomed Mater 2018;88:478.

Appendix

Custom bioreactor

All parts of the bioreactor that came in contact with media/cells were sterilized by autoclave before assembly. The bioreactor consisted of 3 main parts: a pump, a culture chamber, and an oxygenator (Fig. 1b). The pump was a Fisherbrand FH100M Multichannel Peristaltic Pump (Fisher HealthCare, Houston, TX; Cat. No. 13-310-661). Glass bottles with maximum capacity of 100 mL were used as culture chambers, with a perforated lid that serves to connect the inlet and the outlet tubing. An oxygenator was created by coiling approximately 2 meters of silicone tubing, which is permeable to oxygen, and placing it in a plastic bag with a CO_2 source. The culture chamber and oxygenator were kept in the incubator during culture, while approximately 2 feet of tubing extended out of the incubator connecting it to the pump.

Cell preparation and seeding

Early passage human primary dermal fibroblasts (ATCC, Manassa, Virginia; PCS-201-012) were grown to confluence. Cells were grown in Fibroblast Basal Medium (ATCC; PCS-201-030) supplemented with Fibroblast Growth Kit-Low Serum (ATCC; PCS-201-041) and 1% penicillin/streptomycin. Tenocytes were isolated from patellar tendons of Sprague Dawley rats [25]. The tendon samples were collected from the mid portion of the tendons and placed in sterile phosphate-buffered saline solution (PBS). Samples were washed 3 times, then the epitenon layer was removed using a sterile scalpel. The tendon was cut into small pieces (~2-3 mm), then the pieces were placed in 35-mm culture dishes and supplemented with culture medium. The medium was changed every 33 to 4 days. Tenocytes were grown in Dulbecco's Modified Eagle Medium (DMEM)—low glucose (Sigma Aldrich, St. Louis, MO; D6046-500ML) supplemented with 10% fetal bovine serum (FBS) and 1% penicillin/streptomycin. Cells were incubated at 37°C with 5% CO_2, and the medium was changed every 33 to 4 days. When cells reached confluency, they were trypsinized, counted, and diluted to a concentration of approximately 4500 cells per microliter.

Disposable 1-mL syringes were used for cell seeding. Syringes were filled with 0.020 mL of cell suspension (the maximum amount the 400-μm-pore cylinder could hold). Cylinders were directly seeded with fibroblasts or tenocytes (approximately 4500 cells/μl) by injecting the cell suspension using the 1-mL syringes fitted onto one end of the tubing, thus preventing the cells from escaping through the open pores on the surface. The whole syringe/cylinder apparatus was placed horizontally in a sterile dish and incubated for 2-3 hours at 37°C with 5% CO_2 to allow cell attachment. Once incubation was complete, the cylinders, still surrounded in silicone tubing, were cut from the syringe and transferred to the custom-made bioreactor culture chamber and cultured under dynamic conditions (circulating 50 mL of media at 1.3 mL/min) for up to 15 days with full medium change every week. To verify how many cells remained in each cylinder after the transfer, the remaining cells in the tips of each syringe were washed and combined in 1-mL PBS and then counted again to verify approximately the number of cells. Each cylinder held about 200,000 (tenocytes) or 300,000 (fibroblasts) cells on day 0.